Journal of Materials Chemistry C

Accepted Manuscript

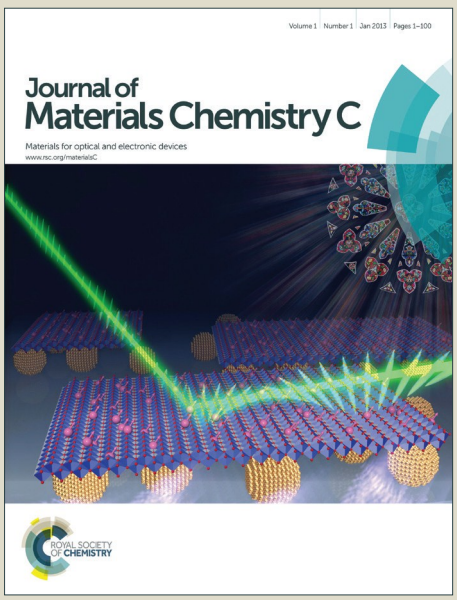

ROYAL SOCIETY OF CHEMISTRY

www.rsc.org/materialsC

Journal of Materials Chemistry C RSCPublishing

ARTICLE

Cite this: DOI: 10.1039/x0xx00000x

Received 00th January 2012,
Accepted 00th January 2012

DOI: 10.1039/x0xx00000x

www.rsc.org/

Aggregation-induced emission enhancement and mechanofluorochromic of α-cyanostilbene functionalized tetraphenyl imidazole derivatives

Yuyang Zhang[a], Huifang Li[a], Gaobin Zhang[a], Xianyun Xu[a], Lin Kong*[a], Xutang Tao[b], Yupeng Tian[a] and Jiaxiang Yang*[a,b]

Three tetraphenyl imidazole derivatives functionalized by α-cyanostilbene unit (**3a-3c**) have been designed and synthesized. Combination of the representative aggregation-induced emission enhancement fluorophore and propeller sharp tetraphenyl imidazole unit in the same molecule achieved the integration of their function. **3a-3c** emitted weakly in dilute organic solvents and show evidently solvatochromic effect caused by the strong intramolecular charge transfer (ICT), which has been confirmed by density functional theory (DFT) calculations. Meanwhile, in solid state, they exhibited obviously fluorescence and stimuli-responsive emission. The main emission peak of compound **3a** was red-shifted from 519 nm to 550 nm after grinding. The reason could be explained that the destruction of the crystalline structure leads to the planarization of molecular conformation or the increased of conjugation.

1. Introduction

Mechanofluorochromic (MFC) materials can change their emission colors under external force stimuli such as grinding, pressing and stretching.[1-12] As a kind of "smart material", MFC materials have received considerable attention because of their fundamental importance and potential applications in memories, anti-counterfeiting of brands, security inks and other optoelectronic devices.[13-22] However, MFC materials are still rare, which may be due to two main reasons.[23-25] First, most conventional luminophores usually suffer from aggregation-caused quenching (ACQ) effects in the solid state, which ultimately limited the development of chromic materials. Secord, the lack of abundant reports on their structure-property relationships of MFC materials has become a main reason of design and synthesis of MFC materials.

Over the past decades, researchers discovered and reported abundant aggregation-induced emission (AIE)[26-38] or aggregation-induced emission enhancement (AIEE)[39-55] materials, which are no luminescence or weak in solution but exhibit strong luminescence in the aggregated state. This phenomenon provides the possibility to obtain high efficiency MFC materials. In addition, investigators have reported some MFC molecules and general mechanisms of chromism are considered to be associated with changes in the molecular packing modes and crystallinities in external environments.[2,14,56] However, the design and synthesis of AIE/AIEE molecules whose molecular packing patterns and intramolecular conformations are easily and reversibly changed by external stimuli is still a challenge.[2]

Herein, based on the predication of structure-property relationships, we designed and synthesized three tetraphenyl imidazole derivatives (**3a-3c**) containing α-cyanostilbene unit by Debus-Radziszewski reaction and Knoevenagel reaction. In recent years, the α-cyanostilbene derivatives have been subsequently developed and they exhibit prominent optical and electrical properties,[39,44,57-64] such as AIEE, high electrical conductivity. So, we modified the imidazole ring with α-cyanostilbene unit to obtain the novel compounds with AIEE property. Meanwhile, we used benzaldehyde with different substituent groups to change the molecular planarity *via* the intramolecular hydrogen bond to investigate the relationship between the molecular structure and properties. In this study, we found that compounds **3a-3c** shown excellent AIEE properties. Meanwhile, **3a** exhibited obviously reversible mechanofluorochromic property in solid state after grinding and fumed with ethanol. Combining the PXRDs and single crystal structures of **3a** and **3b**, the mechanism of mechanofluorochromic properties was analyzed carefully. The result indicated that the destruction of the crystalline structure led to the planarization of molecular conformation or the increased of conjugation degree, which are considered as a

possible reason for the red-shift of fluorescence emission after grinding.[17,20,21,24]

2. Experimental

2.1. Materials and instruments

All of the chemicals and solvents were obtained from the commercial suppliers without further purification. FT-IR spectra were obtained on a Nicolet NEXUS 380 spectrometer (4000-400 cm^{-1}, KBr pellets). ^1H NMR (400 MHz) and ^{13}C NMR (100 MHz) spectra were recorded on a Bruker Avance 400 MHz spectrometer, using DMSO-d_6 or $CDCl_3$ as solvent and tetramethylsilane (TMS) as internal standard. The triple quadrupole mass spectrometer equipped with an electrospray ion source (ESI). The data were obtained by Mass Hunter software. Column chromatography was carried out on silica gel. UV-vis absorption spectra were recorded using a TU-1901 spectrometer from Beijing Purkinje General Instrument Co., Ltd with samples in solution and a quartz cuvette (path length 1 cm). Fluorescence spectra were obtained on Hitachi FL-7000 (Hitachi high technologies corporation Tokyo Japan). The powder X-ray diffraction (PXRD) patterns were recorded on a MXP18AHF diffractometer using Cu Ka radiation (λ = 1.54056 Å) in the 2θ range from 3° to 60°. The absolute photoluminescence quantum yield of solid state was measured on HORIBA FluoroMax-4 spectrofluorometer using an integrating sphere (HORIBA Scientific, F-3092 integrating sphere). The X-ray diffraction measurement of single crystal was performed on a Bruker SMART II CCD area detector using graphite-monochromated Mo Ka radiation. Photo images were obtained using a digital camera (Nikon D7000).

2.2. Synthesis

The chemical structures and synthetic routes of the targeted compounds **3a-3c** are shown in Scheme 1. The detailed procedure was listed as the following.

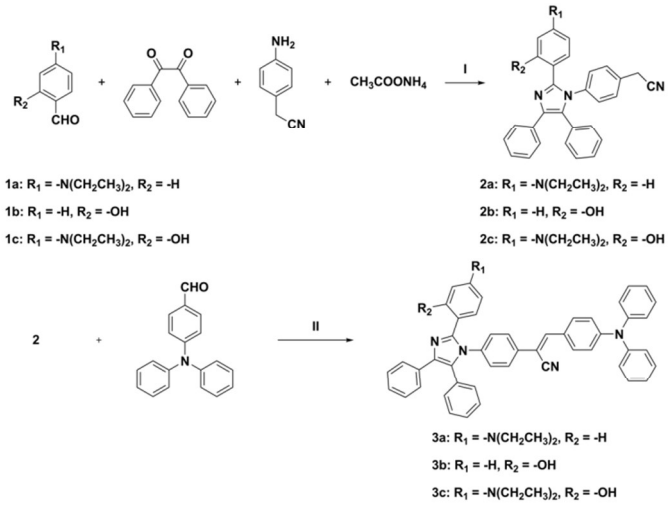

Scheme 1 Synthetic routes of compounds **3a-3c**. Reagents and conditions: (I) acetic acid, 120 °C; (II) *t*-BuOK, ethanol, 80 °C.

2.2.1. Synthesis of compounds 2a-2c

Benzil (0.42 g, 2.0 mmol) and compound **1** (2.0 mmol) were dissolved in acetate acid (20 mL) in room temperature. And compound 2-(4-aminophenyl)acetonitrile (0.40 g, 3.0 mmol) was dissolved in 2 mL acetate acid and was added dropwise in the mixture solution. Two hours later, the ammonium acetate (0.77 g, 10.0 mmol) was added. Then, the mixture was heated at 120 °C. The reaction was monitored by TLC to ensure complete reaction. After termination of the reaction, the resulting mixture was poured into cold water (200 mL) and neutralization with Na_2CO_3. The precipitation was filtered and dried. The compound **2b** was washed with hot ethanol and compounds **2a** and **2c** were recrystallized with ethanol to obtain the pure compounds **2a-2c**.

Compound **2a**: yellow solid, yield 60%. FT-IR (KBr, cm^{-1}): 3051, 2962, 2248, 1611, 1541, 1515, 1484, 1444, 1392, 1356, 1268, 1201, 1069, 825, 697. ^1H NMR (DMSO-d_6, 400 MHz) δ: 1.02-1.04 (t, 6H), 3.26-3.30 (m, 4H), 4.03 (s, 2H), 6.51 (d, 2H, J = 5.24 Hz), 7.11-7.15 (m, 3H), 7.19-7.22 (m, 4H), 7.25-7.29 (m, 7H), 7.43 (d, 2H, J = 5.24 Hz).^{13}C NMR (DMSO-d_6, 100 MHz) δ: 12.38, 21.97, 43.45, 110.46, 116.51, 118.92, 126.19, 126.24, 128.04, 128.26, 128.42, 128.72, 129.33, 130.23, 130.63, 131.14, 131.48, 134.62, 136.32, 136.51, 146.88, 147.16, 156.32.

Compound **2b**: white solid, yield 43%. FT-IR (KBr, cm^{-1}): 3426, 3051, 2968, 2251, 1604, 1581, 1511, 1481, 1412, 1385, 1293, 1254, 1184, 1037, 830, 778, 754, 699. ^1H NMR (DMSO-d_6, 400 MHz) δ: 4.05 (s, 2H), 6.56-6.59 (t, 1H), 6.73 (d, 1H, J = 5.28 Hz), 6.90 (d, 1H, J = 5.44 Hz), 7.15-7.20 (m, 2H), 7.25-7.32 (m, 9H), 7.35 (d, 2H, J = 5.56 Hz), 7.41 (d, 2H, J = 5.00 Hz), 12.19 (s, 1H). ^{13}C NMR (DMSO-d_6, 100 MHz) δ: 22.01, 114.21, 116.81, 118.20, 118.87, 126.09, 126.85, 127.27, 128.39, 128.56, 128.76, 128.92, 129.05, 129.61, 130.26, 130.59, 131.23, 132.19, 133.23, 134.68, 135.91, 144.54, 157.07.

Compound **2c**: yellow solid, yield 36%. FT-IR (KBr, cm^{-1}): 3426, 3051, 2965, 2248, 1632, 1559, 1514, 1463, 1418, 1360, 1271, 1219, 1149, 1069, 778, 694. ^1H NMR (DMSO-d_6, 400 MHz) δ: 1.01-1.03 (t, 6H), 3.23-3.26 (m, 4H), 4.09 (s, 2H), 5.82 (d, 1H, J = 6.04 Hz), 6.14 (s, 1H), 6.29 (d, 1H, J = 6.04 Hz), 7.17-7.19 (t, 1H), 7.23-7.29 (m, 7H), 7.37 (d, 4H, J = 5.48 Hz), 7.41 (d, 2H, J = 5.52 Hz), 13.04 (s, 1H). ^{13}C NMR (DMSO-d_6, 100 MHz) δ: 12.50, 22.06, 43.45, 98.24, 100.72, 102.34, 118.89, 125.92, 126.65, 126.74, 128.38, 128.49, 128.65, 129.11, 129.44, 129.53, 129.68, 131.36, 132.33, 133.15, 133.43, 136.29, 145.69, 148.80, 159.37.

2.2.2. Synthesis of compounds 3a-3c

Compounds **2** (0.5 mmol) and 4-(diphenylamino)benzaldehyde (0.14 g, 0.5 mmol) were dissolved in ethanol (20 mL) at 80 °C, and the *t*-BuOK (0.11 g, 1.0 mmol) was added to the mixture solution subsequently. The reaction was monitored by TLC to ensure complete reaction. After termination of reaction, the yellow precipitate was filtered and washed with the hot ethanol and got pure compounds **3a-3c**.

Compound **3a**: yellow solid, yield 79%. FT-IR (KBr, cm^{-1}): 3051, 2969, 2204, 1610, 1579, 1513, 1490, 1338, 1270, 1192, 1074, 820, 696. ^{1}H NMR ($CDCl_3$, 400 MHz) δ: 1.12-1.15 (t, 6H), 3.30-3.36 (m, 4H), 6.53 (d, 2H, J = 8.52 Hz), 7.03 (d, 2H, J = 8.68 Hz), 7.09-7.19 (m, 11H),7.22-7.34 (m, 11H), 7.39 (s, 1H), 7.53 (d, 2H, J = 8.40 Hz), 7.59 (d, 2H, J = 7.44 Hz), 7.74 (d, 2H, J = 8.68 Hz). ^{13}C NMR ($CDCl_3$, 100 MHz) δ: 12.62, 44.26, 106.39, 111.01, 116.99, 118.56, 120.56, 124.60, 125.87, 125.97, 126.08, 126.44, 127.46, 127.90, 128.10, 128.44, 129.05, 129.63, 129.67, 129.77, 130.11, 130.80, 131.21, 134.43, 134.68, 137.71, 138.06, 142.29, 146.48, 147.71, 147.86, 150.25. MS (ESI+, 4.5 kV, 200 °C): m/z = 738.3605 ($[M+H]^+$), calcd for $C_{52}H_{43}N_5^+$ = 737.3518 (M^+).

Compound **3b**: yellow solid, yield 82%. FT-IR (KBr, cm^{-1}): 3431, 3061, 2206, 1583, 1506, 1488, 1384, 1332, 1295, 1255, 1179, 753, 698. ^{1}H NMR (DMSO-d_6, 400 MHz) δ: 6.48-6.52 (t, 0.38H), 6.56 (d, 0.76H, J = 8.68 Hz), 6.62-6.66 (t, 0.63H), 6.74 (d, 0.76H, J = 8.64 Hz), 6.81-7.01 (m, 4.09H), 7.09-7.46 (m, 23.78H), 7.69 (d, 1.31H, J = 8.36 Hz), 7.83 (d, 1.26H, J = 8.68 Hz), 7.94 (s, 0.64 H), 11.94 (s, 0.36H), 12.10 (s, 0.61H). ^{13}C NMR (DMSO-d_6, 100 MHz) δ: 104.88, 107.16, 114.34, 114.50, 116.64, 116.77, 118.09, 118.14, 118.20, 118.35, 119.59, 120.36, 124.57, 124.80, 125.15, 125.71, 125.75, 125.94, 126.01, 126.14, 126.23, 126.82, 126.87, 127.55, 127.66, 128.37, 128.61, 128.78, 129.19, 129.51, 129.60, 129.73, 129.87, 129.95, 130.23, 130.32, 130.53, 130.58, 130.95, 131.23, 131.26, 131.37, 133.25, 133.98, 134.56, 134.85, 134.89, 136.52, 137.18, 143.31, 144.53, 144.59, 144.89, 145.71, 145.88, 149.28, 149.73, 156.90, 156.97. MS (ESI+, 4.5 kV, 200 °C): m/z = 683.2816 ($[M+H]^+$), calcd for $C_{48}H_{34}N_4O^+$ = 682.2733 (M^+).

Compound **3c**: yellow solid, yield 78%. FT-IR (KBr, cm^{-1}): 3432, 3059, 2968, 2210, 1623, 1581, 1508, 1489, 1333, 1272, 1178, 696. ^{1}H NMR ($CDCl_3$, 400 MHz) δ: 1.12-1.15 (t, 6H), 3.28-3.33 (m, 4H), 5.86 (d, 1H, J = 7.24 Hz), 6.34 (s, 1H), 6.38 (d, 1H, J = 8. 96 Hz), 7.04 (d, 2H, J = 8.80 Hz), 7.13-7.25 (m, 16H), 7.31-7.35 (t, 4H), 7.44 (s, 1H), 7.53 (d, 2H, J = 7.12 Hz), 7.62 (d, 2H, J = 8.44 Hz), 7.77 (d, 2H, J = 8.80 Hz), 13.42 (s, 1H). ^{13}C NMR ($CDCl_3$, 100 MHz) δ: 12.74, 44.21, 99.12, 102.57, 106.10, 118.50, 119.85, 120.45, 124.67, 124.77, 125.81, 125.93, 126.03, 126.48, 126.72, 126.77, 126.89, 126.98, 128.21, 128.35, 128.39, 128.55, 129.46, 129.64, 129.68, 129.89, 130.18, 130.90, 131.29, 131.43, 131.51, 142.71, 146.43, 150.41. MS (ESI+, 4.5 kV, 200 °C): m/z = 754.3553 ($[M+H]^+$), calcd for $C_{52}H_{43}N_5O^+$ = 753.3468 (M^+).

3. Results and discussion

3.1. Synthesis

The compounds **2a-2c** were synthesized by Debus-Radziszewski reaction referring to the literature.[65] The compounds **2a-2c** were characterized by FT-IR, ^{1}H NMR and ^{13}C NMR spectra. Targeted compounds **3a-3c** were synthesized *via* Knoevenagel reaction and characterized by FT-IR, ^{1}H NMR, ^{13}C NMR, MS spectroscopic techniques and X-ray crystallographic structures as described in Fig. 4.

3.2. Solvatochromic effect

The UV-vis and fluorescence spectra of the compounds **3a-3c** in different solvents (toluene, benzene, dichloromethane (DCM), tetrahydrofuran (THF), ethanol (EtOH), ethyl acetate (EA), chloroform, acetonitrile, *N*, *N*-dimethylformamide (DMF), methanol, dimethyl sulfoxide (DMSO)) are shown in Fig. 1, Fig. S1, Fig. S2 and the corresponding photophysical data are summarized in Table S1. As we know, the solvents can change the energy levels of the absorption or emission bands. As depicted in Fig. 1 and Fig. S1, compounds **3a** and **3b** show two characteristic absorption bands at about 300 nm and 400 nm in varying solvents, which are attributed to the π-π* and intramolecular charge transfer (ICT) transitions, respectively.[66-67] While, **3c** shows three absorption bands at about 300 nm, 335 nm and 400 nm, the two main energy absorption bands were attributed to π-π* transitions, and the low energy absorption band originated from ICT transition. For fluorescent spectra (Fig. 1, Fig. S1 and Fig. S2), we can obviously observed that the emission wavelengths of compounds **3a-3c** red-shifted and quenched at the same time with increasing polarity of the solvent. The emission maximum of **3a-3c** exhibited bathochromic shifts of 63 nm, 49 nm and 69 nm from toluene to acetonitrile, respectively. To have a better insight into the ICT process, the density functional of B3LYP with 6-31G* basis sets were used to investigate the electron cloud distribution (Fig. S3). The electron cloud distributions of **3a-3c** were similar. The electron cloud of highest occupied molecular orbital (HOMO) was mainly localized on the imidazole ring, different substituent groups and benzene ring of 2 position of imidazole ring. For the other segments, only a small amount of electron cloud distribution. In addition, the HOMO-LUMO gap for **3c** is smaller than for **3a** and **3b**, match with the trend observed in the absorption properties. Meanwhile, the lowest unoccupied molecular orbital (LUMO) was localized on the α-cyanostilbene unit due to strong electron-withdrawing ability of cyanogroup. Compounds **3a-3c** exhibited obviously charge separation and indicated a typical intramolecular charge transfer (ICT) effect.[67]

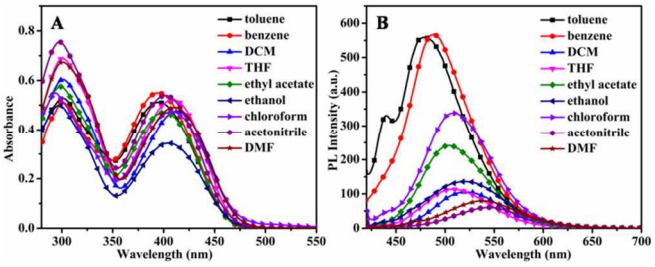

Fig. 1. The UV-vis spectra (A) and fluorescence spectra (B) of compound **3a** in different solvents (1×10^{-5} mol·L^{-1}).

3.3. Aggregation-induced emission enhancement performances

Compounds **3a-3c** are soluble in common organic solvents in low concentration, such as ethanol, THF, ethyl acetate and almost insoluble in water. To investigate the AIE or AIEE characteristic of **3a-3c**, their UV-vis and fluorescent spectra with different fraction of water were studied (Fig. 2, Fig. S4 and Fig. S5). The concentrations of **3a-3c** were kept at 1×10^{-5} mol·L^{-1}. For UV-vis spectra of compound **3a** (Fig. 2), with an increasing fraction of water from 0 to 30%, the absorption band almost remained at the same position of

405 nm. With up to 40% of water content, **3a** molecules began to form aggregates, and the absorption band showed an obvious red-shift. The possible reasons are that the increase of the polarity and the planarization of a twisted molecule caused the extension of the effective conjugation lengths in the aggregated state.[47,68-69] Meanwhile, the formation of aggregates was speculated from the level-off tail in the UV-vis spectra when the water volume fraction was 40% to 99%. These tails are attributed to Mie scattering caused by nanosized particles.[70-71]

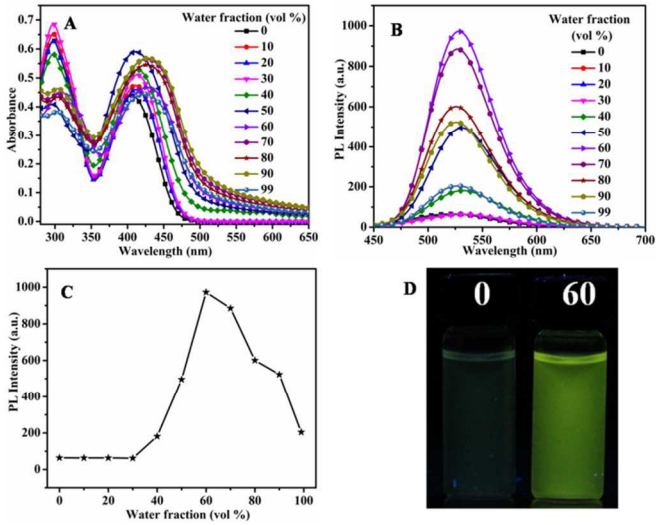

Fig. 2. The UV-vis absorption (A) and fluorescence spectra (B) of compound **3a** in ethanol-water mixtures with different water volume fractions; the effect of water volume fraction on the maximum emission intensity (C); optical photographs recorded under 365 nm UV irradiation with various fractions of water (D).

For the fluorescence intensity, compound **3a** showed a dramatic change from weakly emitting in monomolecular state to strongly fluorescent in aggregate state (Fig. 2). When the water fraction is inferior to 30%, the fluorescence intensity of compound **3a** emitted weakly fluorescence emission, whereas in the case of 40% volume fractions of water addition, the molecule began aggregating and the fluorescence intensity promptly increased and reached the maximum value at 60%. Meanwhile, we can see that the nanoparticles exhibit an enhancement of green-yellow emission under UV illumination. The mechanism of aggregation-induced emission enhancement may be attributed to the restriction of intramolecular rotation (RIR) and intermolecular interaction.[72-74] When fraction of water is higher than 60%, the fluorescence intensity gradually decreases. This phenomenon is reasonable that aggregates commenced to form and precipitate quickly at high water content. This process leads to the decrease of effectively fluorescent species and lowers the fluorescence intensity. Moreover, as shown in Fig. S4 and Fig. S5, we found that compounds **3b** and **3c** displayed a similar behavior. The fluorescence intensity of **3a-3c** in the aggregated state were obviously stronger than that of the ethanol solution, the emission intensity were 15.2, 5.4 and 3.3 fold, respectively. It is worth noting that the multiple of **3a** is obviously stronger than **3b** and **3c**. Combining with the single crystal structures of **3a** and **3b** (Fig. 4), we found that **3a** exhibited a large number of intermolecular interactions in whole molecule moiety. However, intermolecular interactions of **3b** were just focus on the imidazole ring and benzene rings of 1, 2, 4 and 5 positions. It indicated that the intramolecular rotations suffered stronger restriction for **3a** in the aggregated state. It may be the main reason that **3a** showed greater multiples of fluorescence emission intensity. All of phenomena showed that compounds **3a-3c** were an AIEE-active material.

3.4. Mechanofluorochromic properties

The AIEE feature and high quantum yields in solid state may be suggested that those compounds may be as stimuli responsive smart materials. To check whether compounds **3a-3c** are mechanofluorochromic properties, their UV-vis and emission properties were studied in solid state. While compounds were purified *via* washing with hot ethanol and exhibited strong green emission at 519 nm for **3a** and yellowish-green at 539 nm, 537 nm for **3b**, **3c** and quantum yields were 0.11, 0.37, 0.15, respectively (Table S1). They emit yellow lights after grinding with a spatula for 5 min. As shown in Fig. 3, Fig. S8 and Fig. S9, the emission peaks occur obvious red shift for **3a-3c** from 519 to 550 nm, 539 to 549 nm and 537 nm to 550 nm, respectively. When fuming with ethanol vapor for 2 min, compounds **3a-3c** almost returned to the original fluorescence emission. For the UV-vis spectra of **3a-3c** in different solid states (Fig. S6), it was found that the maximum absorption peaks of solid state occurred obviously red-shift compared with in dilute solution, it mainly reason is that the effectively conjugation increased through intermolecular interaction in solid state. Meanwhile, for **3a** and **3c**, the absorption peak appeared red-shift after grinding (from 435 nm to 448 nm for **3a**, from 433 nm to 447 nm for **3c**), which suggested that the molecular conformation become more planarization and further increased the conjugation degree. The results indicated that the pressure of the grinding changes not only the absorption spectra but also the emission spectra. In addition, we investigated the reversible cycle process of compound **3a** (Fig. S7). The results show that the conversion between the green and yellow emission can be repeated many times without fatigue due to the nondestructive nature of the stimuli.[2,14]

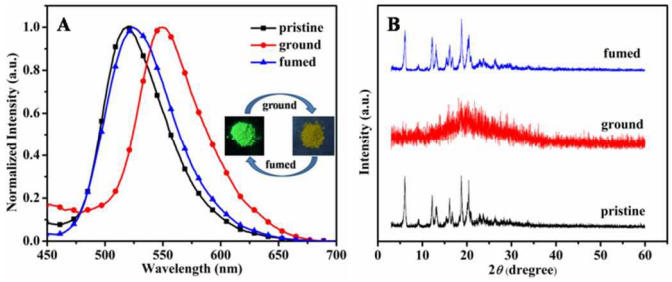

Fig. 3. Emission spectra (A) and PXRD patterns (B) of pristine, ground and fumed with ethanol of compound **3a**. Inset: photographs of pristine and ground powers under 365 nm light.

To gain the mechanism of mechanofluorochromic properties, the powder X-ray diffraction (PXRD) analysis was conducted. Meanwhile, the pristine powders **3a-3c** exhibit much intense and sharp diffraction and the ground powders show rather weak signals,

indicating the molecular packing from regular crystalline nature to disordered.[18,20,21] However, when the ground powders were fumed with ethanol, the sharp diffraction peaks arise again, implying those compounds recover to ordered crystalline state.

Table 1 Summary of crystallographic data and structure refinement details for compounds **3a** and **3b**

Identification code	**3a**	**3b**
Empirical formula	$C_{52}H_{43}N_5$	$C_{48}H_{34}N_4O$
Formula weight	737.91	682.79
Temperature	293(2) K	296(2) K
Wavelength	0.71069 Å	0.71073 Å
Crystal system	Monoclinic	Triclinic
space group	P2(1)/c	pī
a	14.689(5) Å	9.8096(14) Å
b	18.897(5) Å	14.224(2) Å
c	15.282(5) Å	14.627(2) Å
α	90.000(5) °	88.198(2) °
β	98.117(5) °	83.699(2) °
γ	90.000(5) °	71.647(2) °
Volume	4199(2) $Å^3$	1925.5(5) $Å^3$
Z, Calculated density	4, 1.167 Mg/m^3	2, 1.178 Mg/m^3
Absorption coefficient	0.069 mm^{-1}	0.071 mm^{-1}
F(000)	1560	716
Theta range for data collection	1.40 to 25.00 °	1.40 to 25.00 °
Limiting indices	-17≤h≤17, -21≤k≤22, -18≤l≤17	-11≤h≤11, -16≤k≤16, -17≤l≤16
Reflections collected/unique	29562/7389 [R (int) = 0.0929]	13810 / 6708 [R(int) = 0.0473]
Max. and min. transmission	0.9877 and 0.9864	0.9873 and 0.9866
Data/restraints/parameters	7389/6/516	6708 / 0 / 479
Goodness-of-fit on F^2	0.940	1.193
Final R indices [I>2sigma(I)]	R_1 = 0.0614 wR_2 = 0.1481	R_1 = 0.0784 wR_2 = 0.2192
R indices (all data)	R_1 = 0.1589 wR_2 = 0.2073	R^1 = 0.1605 wR^2 = 0.2577

To further investigate the phase transition in the procedure of MFC phenomenon, differential scanning calorimetry (DSC) measurements were conducted at pristine and ground state (Fig. S10). DSC results showed that the ground powders of **3a-3c** exhibited clear exothermic transition peaks at 155.8 °C, 154.5 °C, 156.7 °C, respectively, whereas, no exothermic peaks were observed for the pristine powders at same temperature. It suggested that the molecular conformation and intermolecular arrangements have been changed and formed metastable states after grinding, which were responsible to the mechanofluorochromic behaviors. In addition, the high transformation temperatures indicated that the ground powders were stabilized and can still remain metastable state at room temperature.

The lifetime data are illustrated in Fig. S11. Fluorescence decay experiments show that **3a** in the crystalline state has a longer lifetime than in the amorphous state. The obviously changes in lifetime (from 0.66 ns to 0.1 ns) indicated that the molecular aggregation structures have significant change, suggest that the intermolecular interactions were destroy after grinding. For **3b** and **3c**, the lifetime show small changes (from 0.55 ns to 0.61 ns for **3b**, from 1.31 ns to 0. 76 ns for **3c**), indicated the molecular stacking just showed small change after grinding. The experimental results were also matched with the fluorescence changes.

It is worth noting that the compound **3a** exhibited greater red shift than **3b** and **3c** after grinding. In order to further analysis the mechanofluorochromic mechanisms. The optimized molecular structures, crystal structures and crystallographic data collection parameters of **3a** and **3b** were investigated carefully (Fig. S12, Fig. 4, Table 1, Table S2, Table S3, Table S4 and Table S5). Suitable single crystals of **3a** and **3b** for X-ray structural analysis were obtained by slow evaporation of a dichloromethane solution at room temperature for several days. Compound **3a** crystallized in a monoclinic form with the space group P2(1)/c. The crystal packing is stabilized by intermolecular hydrogen bond interactions and C-H···π with its neighbor molecules. The hydrogen bond distance is 2.741 (Å) and the C(29, 42)-H···π bond distances are 2.934(Å), 2.937(Å), respectively. The dihedral angles are 17.69° (C6-C10, C11N2C12C19N3) and 52.37° (C26-C31, C35-C40), respectively. For the optimized molecular structures of **3a**, the dihedral angles are 29.16° (C6-C10, C11N2C12C19N3) and 31.43° (C26-C31, C35-C40), respectively. The molecule exhibited better planarity in crystal than monomolecular state for imidazole ring segment. Meanwhile, the dihedral angles of α-cyanostilbene unit also showed obviously changes. For the optimized molecular structures of **3b**, the dihedral angles are 20.14° (C1-C6, C7N1C8C15N2) and 32.96° (C22-C27, C31-C36), respectively. The mainly reason is that intermolecular interactions restrict the rotation of intramolecular single bonds in solid state. When the intermolecular interactions were destroyed and caused the change of molecular structure. So, the fluorescence emission peak showed obviously different after grinding.

Compound **3b** crystallized in a triclinic form with the space group pī and the crystal was packing by intramolecular hydrogen bond interactions and C-H···π with its neighbor molecules. The C(26, 23, 21, 20, 17, 2)-H···π bond distances are 3.013, 2.913, 3.132, 3.128, 2.700, 3.243 (Å), respectively. Due to the intramolecular hydrogen bond, the dihedral angles are just 2.57° (C1-C6, C7N1C8C15N2) and 39.72° (C22-C27, C31-C36), respectively. The results indicated that **3b** possessed good planarity, which permitted effective conjugation and resulted in a red shifted emission than **3a.** In addition, compound **3a** exhibited greater distortion of molecular structure and can more easily leads to the planarization of molecular conformation than **3b** and **3c**. It may be the main reason that **3a** can more easily change fluorescence emission after grinding.

Journal of Materials Chemistry C RSCPublishing

ARTICLE

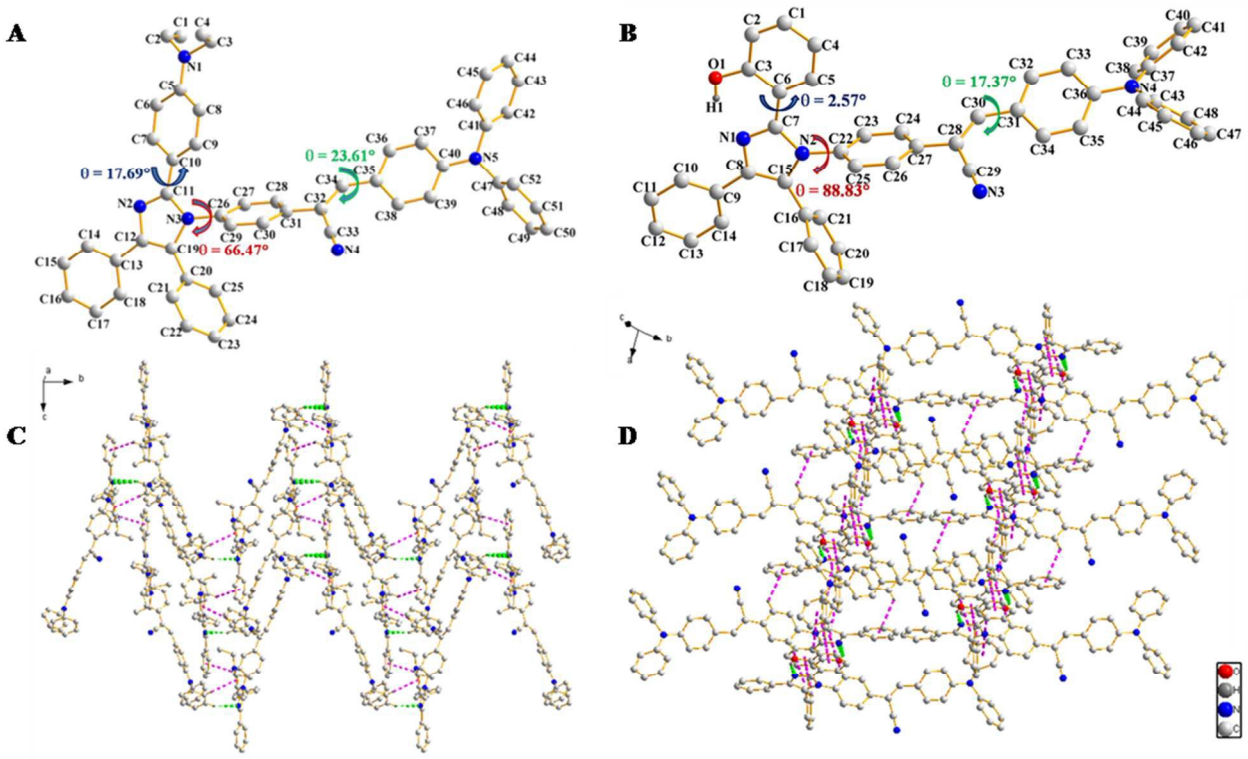

Fig. 4. Crystal structures of compounds **3a** (A) and **3b** (B), intermolecular interactions of **3a** (C) and **3b** (D) (Hydrogen atoms are omitted for the sake of clarity).

4. Conclusions

In summary, three tetraphenyl imidazole derivatives functionalized by α-cyanostilbene unit (**3a-3c**) were synthesized by Debus-Radziszewski and Knoevenagel reaction. The molecules exhibit obviously solvatochromic effect due to the strong intramolecular charge transfer (ICT). In addition, compounds **3a-3c** exhibited aggregation-induced emission enhancement (AIEE) properties attributed to the restriction of intramolecular rotation (RIR) and intermolecular interaction. Meanwhile, the emission peak of compounds **3a** shows obviously red-shifted than **3b** and **3c** after grinding. The mechanofluorochromic mechanisms were investigated carefully according to PXRD and crystal structures. Our investigation shows that the destruction of the crystalline structure leads to the planarization of molecular conformation or the increased of conjugation degree, which is considered as a possible reason for the red-shift of fluorescence emission.

Acknowledgements

This work was supported by the Educational Commission of Anhui Province of China (KJ2014ZD02) and the National Natural Science Foundation of China (51432001).

Notes and references

[a]*Department of Chemistry, Anhui University and Key Laboratory of Functional Inorganic Materials of Chemistry of Anhui Province, Hefei 230039, P. R. China. E-mail: jxyang@ahu.edu.cn; kong_lin2009@126.com*

[b]*State Key Laboratory of Crystal Materials, Shandong University, Jinan 250100, P. R. China.*

† Electronic Supplementary Information (ESI) available: UV-vis absorption and PL in different polarity solvents of **3b** and **3c**; the volume fractions of water effect on the absorption and fluorescence spectra in ethanol-water mixtures; DFT calculations; Crystal data and details of **3a** and **3b**; CCDC 1037346, 1042261. See DOI: 10.1039/b000000x/

1 G. H. Zhang, J. B. Sun, P. C. Xue, Z. Q. Zhang, P. Gong, J. Peng and R. Lu. *J. Mater. Chem. C*, 2015, **3**, 2925.
2 C. X. Niu, Y. You, L. Zhao, D. C. He, N. Na and J. Ouyang. *Chem. Eur. J.*, 2015, **21**, 13983.
3 H. W. Sun, Y. Zhang, W. Yan, W.X. Chen, Q. Lan, S. W. Liu, L. Jiang, Z. G. Chi, X. D. Chen and J. R. Xu. *J. Mater. Chem. C*, 2014, **2**, 5812.
4 X. Q. Wang, Q. S. Liu, H. Yan, Z. P. Liu, M. G. Yao, Q. F. Zhang, S. W. Gong and W. J. He. *Chem. Commun.*, 2015, **51**, 7497.
5 Z.Q. Zhang, Z. Wu, J. B. Sun, B. Q. Yao, G. H. Zhang, P. C. Xue and R. Lu. *J. Mater. Chem. C*, 2015, **3**, 4921.
6 J. Kunzelman, M. Kinami, B. R. Crenshaw, J. D. Protasiewicz and C. Weder. *Adv. Mater.*, 2008, **20**, 119.
7 Z. Mao, Z. Y. Yang, Y. X. Mu, Y. Zhang, Y. F. Wang, Z. G. Chi, C. C. Lo, S. W. Liu, A. Lien and J. R. Xu. *Angew. Chem. Int. Ed.*, 2015, **54**, 1.
8 Y. Ooyama and Y. Harima, *J. Mater. Chem.*, 2011, **21**, 8372.
9 L. Y. Bu, M. X. Sun, D. T. Zhang, W. Liu, Y. L. Wang, M. Zheng, S. F. Xue and W. J. Yang. *J. Mater. Chem. C*, 2013, **1**, 2028-2035.
10 X. Q. Zhang, Z. G. Chi, H. Y. Li, B. J. Xu, X. F. Li, W. Zhou, S. W. Liu, Y. Zhang and J. R. Xu. *Chem. Asian J.*, 2011, **6**, 808-811.
11 Q. K. Qi, Y. F. Liu, X. F. Fang, Y. M. Zhang, P. Chen, Y. Wang, B. Yang, B. Xu, W. J. Tian and S. X. A. Zhang. *RSC Adv.*, 2013, **3**, 7996-8002.
12 X. Q. Zhang, Z. G. Chi, J. Y. Zhang, H. Y. Li, B. J. Xu, X. F. Li, S. W. Liu, Y. Zhang and J. R. Xu. *J. Phys. Chem. B*, 2011, **115**, 7606-7611.
13 Q. B. Song, Y. S. Wang, C.C. Hu, Y. J. Zhang, J. W. Sun, K. Y. Wang and C. Zhang. *New J. Chem*., 2015, **39**, 659.
14 M Tanioka, S. Kamino, A. Muranaka, Y. Ooyama, H. Ota, Y. Shirasaki, J. Horigome, M. Ueda, M. Uchiyama, D. Sawada and S. Enomoto. *J. Am. Chem. Soc.*, 2015, **137**, 6436.
15 H. Y. Li, Z. G. Chi, B. J. Xu, X. Q. Zhang, X. F. Li, S. W. Liu, Y. Zhang and J. R. Xu, *J. Mater. Chem.*, 2011, **21**, 3760.
16 B. J. Xu, M. Y. Xie, J. J. He, B. Xu, Z. G. Chi, W. J. Tian, L. Jiang, F. L. Zhao, S. W. Liu, Y. Zhang, Z. Z. Xu and J. R. Xu. *Chem. Commun.*, 2013, **49**, 273.
17 H. Y. Li, X. Q. Zhang, Z. G. Chi, B. J. Xu, W. Zhou, S. W. Liu, Y. Zhang and J. R. Xu. *Org. Lett.*, 2011, **13**, 556.
18 J. Q. Tong, Y. J. Wang, J. Mei, J. Wang, A. J. Qin, J. Z. Sun and B. Z. Tang. *Chem. Eur. J.*, 2014, **20**, 4661.
19 T. Jadhav, B. Dhokale and R. Misra. *J. Mater. Chem. C*, 2015, **3**, 9063.
20 Q. K. Qi, J. B. Zhang, B. Xu, B. Li, S. X. A. Zhang and W. J. Tian, *J. Phys. Chem. C*, 2013, **117**, 24997.
21 Y. J. Zhang, Q. B. Song, K. Wang, W. G. Mao, F. Cao, J. W. Sun, L. L. Zhan, Y. K. Lv, Y. G. Ma, B. Zou and C. Zhang, *J. Mater. Chem. C*, 2015, **3**, 3049.
22 J. Wang, J. Mei, R. R. Hu, J. Z. Sun, A. J. Qin and B. Z. Tang, *J. Am. Chem. Soc.*, 2012, **134**, 9956.
23 X. Q. Zhang, Z. Y. Ma, Y. Yang, X. Y. Zhang, X. R. Jia and Y. Wei. *J. Mater. Chem. C*, 2014, **2**, 8932.
24 Z. G. Chi, X. Q. Zhang, B. J. Xu, X. Zhou, C. P. Ma, Y. Zhang. S. W. Liu and J. R. Xu, *Chem. Soc. Rev.*, 2012, **41**, 3878.
25 X. F. Mei, G. X. Wen, J. W. Wang, H. M. Yao, Y. Zhao, Z. H. Lin and Q.D. Ling. *J. Mater. Chem. C*, 2015, **3**, 7267.
26 J. D. Luo, Z. L. Xie, J. W. Y. Lam, L. Cheng, H. Y. Chen, C. F. Qiu, H. S. Kwok, X. W. Zhan, Y. Q. Liu, D B. Zhu and B. Z. Tang. *Chem. Commun.*, 2001, 1740.
27 Z. L. Xie, C. J. Chen, S. D. Xu, J. Li, Y. Zhang, S. W. Liu, J. R. Xu and Z. G. Chi. *Angew. Chem.*, 2015, **127**, 7287.
28 J. Zhou, Z. F. Chang, Y. B. Jiang, B. R. He, M. Du, P. Lu, Y. N. Hong, H. S. Kwok, A. J. Qin, H. Y. Qiu, Z. J. Zhao and B. Z. Tang. *Chem. Commun.*, 2013, **49**, 2491.
29 Z. F. Chang, Y. B. Jiang, B. R. He, J. Chen, Z. Y. Yang, P. Lu, H. S. Kwok, Z. J. Zhao, H. Y. Qiu and B. Z. Tang. *Chem. Commun.*, 2013, **49**, 594.
30 Y. Zhang, J. H. Wang, J. Zheng and D. Li. *Chem. Commun.*, 2015, **51**, 6350.
31 P. Galer, R. C. Korosec, M. Vidmar and B. Sket. *J. Am. Chem. Soc.*, 2014, **136**, 7383.
32 R. R. Wei, P. S. Song and A. J. Tong. *J. Phys, Chem. C*, 2013, **117**, 3467.
33 E. Zhao, J. W. Y. Lam, Y. N. Hong, J. Z. Liu, Q. Peng, J. H. Hao, H. H. Y. Sung, I. D. Williams and B. Z. Tang. *J. Mater. Chem. C*, 2013, **1**, 5661.
34 Z. Y. Yang, W. Qin, J. W. Y. lam, S. J. Chen, H. H. Y. Sung, I. D. Williams and B. Z. Tang. *Chem. Sci.*, 2013, **4**, 3725.
35 Z. T. Luo, X. Yuan, Y. Yu, Q. B. Zhang, D. T. Leong, J. Y. Lee and J. P. Xie. *J. Am. Chem. Soc.*, 2012, **134**, 16662.
36 J. Huang, N. Sun, Y. Q. Dong, R. L. Tang, P. Lu, P. Cai, Q. Q. Li, D. G. Ma, J. G. Qin and Z. Li. *Adv. Funct. Mater.*, 2013, **23**, 2329.
37 Q. S. Li and L. Blancafort. *Chem. Commun.*, 2013, **49**, 5966-5968.
38 Z. Zheng, Z. P. Yu, M. D. Yang, F. Jin, Q. Zhang, H. P. Zhou, J. Y. Wu and Y. P. Tian. *J. Org. Chem.*, 2013, **78**, 3222-3234.
39 B. K. An, S. K. Kwon, S. D. Jung and S. Y. Park. *J. Am. Chem. Soc.*, 2002, **124**, 14410.
40 H. Y. Li, Z. G. Chi, B. J. Xu, X. Q. Zhang, X. F. Li, S. W. Liu, Y. Zhang and J. R. Xu. *J. Mater. Chem. C*, 2011, **21**, 3760.
41 H. Y. Li, Z. G. Chi, X. Q. Zhang, B. J. Xu, S. W. Liu, Y. Zhang and J. R. Xu. *Chem. Commun.*, 2011, **47**, 11273.
42 W. B. Wu, S. H. Ye, L. J. Huang, L. Xiao, Y. J. Fu, Q. Huang, G. Yu, Y. Q. Liu, J. G. Qin, Q. Q. Li and Z. Li. *J. Mater. Chem.*, 2012, **22**, 6374.
43 X. Q. Zhang, Z. G. Chi, B. J. Xu, C. J. Chen, X. Zhou, Y. Zhang, S. W. Liu and J. R. Xu. *J. Mater. Chem.*, 2012, **22**, 18405.
44 L. L. Zhu and Y. L. Zhao. *J. Mater. Chem. C*, 2013, **1**, 1059.
45 R. Hu, S. Y. Li, Y. Zeng, J. P. Chen, S. Q. Wang, Y. Li and G. Q. Yang. *Phys. Chem. Chem. Phys.*, 2011, **13**, 2044.
46 W. Huang, F. S. Tang, B. Li, J. H. Su and H. Tian. *J. Mater. Chem. C*, 2014, **2**, 1141.
47 W. B. Jia, H. W. Wang, L. M. Yang, H. B. Lu, L. Kong, Y. P. Tian, X. T. Tao and J. X. Yang. *J. Mater. Chem. C*, 2013, **1**, 7092.
48 Y. Kubota, Y. Ozaki, K. Funabiki and M. Matsui. *J. Org. Chem.*, 2013, **78**, 7058.
49 A. Maity, F. Ali, H. Agarwalla, B. Anothumakkool and A. Das. *Chem. Commun.*, 2015, **51**, 2130.
50 W. Huang, H. Wang, L. Sun, B. Li, J. H. Su and H. Tian. *J. Mater. Chem. C*, 2014, **2**, 6843.
51 L. Kong, Y. P. Tian, Q. Y. Chen, Q. Zhang, H. Wang, D. Q. Tan, Z. M. Xue, J. Y. Wu, H. P. Zhou and J. X. Yang. *J. Mater. Chem. C*, 2015, **3**, 570.

52 S. Kaur, A. Gupta, V. Bhalla and M. Kumar. *J. Mater. Chem. C*, 2014, **2**, 7356.
53 T. He, X. T. Tao, J. X. Yang, D. Guo, H. B. Xia, J. Jia and M. H. Jiang. *Chem. Commun.*, 2011, **47**, 2907.
54 S. J. Ananthakrishnan, E. Varathan, V. Subramanian, N. Somanathan and A. B. Mandal. *J. Phys. Chem. C*, 2014, **118**, 28084.
55 X. B. Du, J. Qi, Z. Q. Zhang, D. G. Ma and Z. Y. Wang. *Chem. Mater.*, 2012, **24**, 2178.
56 R. H. Li, S. Z. Xiao, Y. Li, Q. F. Lin, R. H. Zhang, J. Zhao, C. Y. Yang, K. Zou, D. S. Li and T. Yi. *Chem. Sci.*, 2014, **5**, 3922.
57 B. K. An, J. Gierschner and S. Y. Park. *Acc. Chem. Res.*, 2012, **45**, 544.
58 V. Palakollu and S. Kanvah. *RSC Adv.*, 2015, **5**, 33049.
59 Y. J. Zhang, G. L. Zhuang, M. Ouyang, B. Hu, Q. B. Song, J. W. Sun, C. Zhang, C. Gu, Y. X. Xu and Y. G. Ma. *Dyes Pigm*., 2013, **98**, 486.
60 S. J. Yoon, J. W. Chung, J. Gierschner, K. S. Kim, M. G. Choi, D. Kim and S. Y. Park. *J. Am. Chem. Soc.*, 2010, **132**, 13675.
61 Y. Z. Jin, Y. J. Xia, S. Wang, L. Yan, Y. Zhou, J. Fan and B. Song. *Soft Matter*, 2015, **11**, 798.
62 V. Palakollu and S. Kanvah. *New J. Chem.*, 2014, **38**, 5736.
63 Y. J. Zhang, K. Wang, G. L. Zhuang, Z. Q. Xie, C. Zhang, F. Cao, G. X. Pan, H. F. Chen, B. Zou and Y. G. *Ma. Chem. Eur. J.*, 2015, **21**, 2474.
64 S. Shin, S. H. Gihm, C. R. Park, S. Kim and S. Y. Park. *Chem. Mater.*, 2013, **25**, 3288.
65 S. Park, J. E. Kwon, S. H. Kim, J. Seo, K. Chuang, S. Y. Park, D. J. Jang, B. M. Medina, J. Gierschner and S. Y. Park. *J. Am. Chem. Soc.*, 2009, **131**, 14043.
66 A. X. Ding, L. M. Yang, Y. Y. Zhang, G. B. Zhang, L. Kong, X. J. Zhang, Y. P. Tian, X. T Tao and J. X Yang. *Chem. Eur.* J., 2014, **20**, 12215.
67 Z. R. Grabowski and K. Rotkiewicz. *Chem. Rev.*, 2003, **103**, 3899.
68 M. Levitus, K. Schmieder, H. Ricks, K. D. Shimizu, U. H. F. Bunz and M. A. G. Garibay. *J. Am. Chem. Soc.*, 2001, **123**, 4259.
69 H. Tong, Y. N. Hong, Y. Q. Dong, Y. Ren, M. Haussler, J. W. Y. Lam, K. S. Wong and B. Z. Tang. *J. Phys. Chem. B*, 2007, **111**, 2000.
70 H. Auweter, H Haberkorn, W. Heckmann, D. Horn, E. Luddeche, J. Rieger and H. Weiss. *Angew. Chem. Int. Ed.*, 1999, **38**, 2188.
71 X. Q. Zhang, Z. G. Chi, B. J. Xu, L. Jiang, X. Zhou, Y. Zhang, S. W. Liu and J. R. Xu. *Chem. Commun.*, 2012, **48**, 10895.
72 Y. N. Hong, J. W. Y. Lam and B. Z. Tang. *Chem. Commun.*, 2009, 4332.
73 G. D. Liang, J. W. Y. Lam, W. Qin, J. Li, N. Xie and B. Z. Tang. *Chem. Commun.*, 2014, **50**, 1725.
74 Q. Peng, Y. P. Yi, Z. G. Shuai and J. S. Shao. *J. Am. Chem. Soc.*, 2007, **129**, 9333.

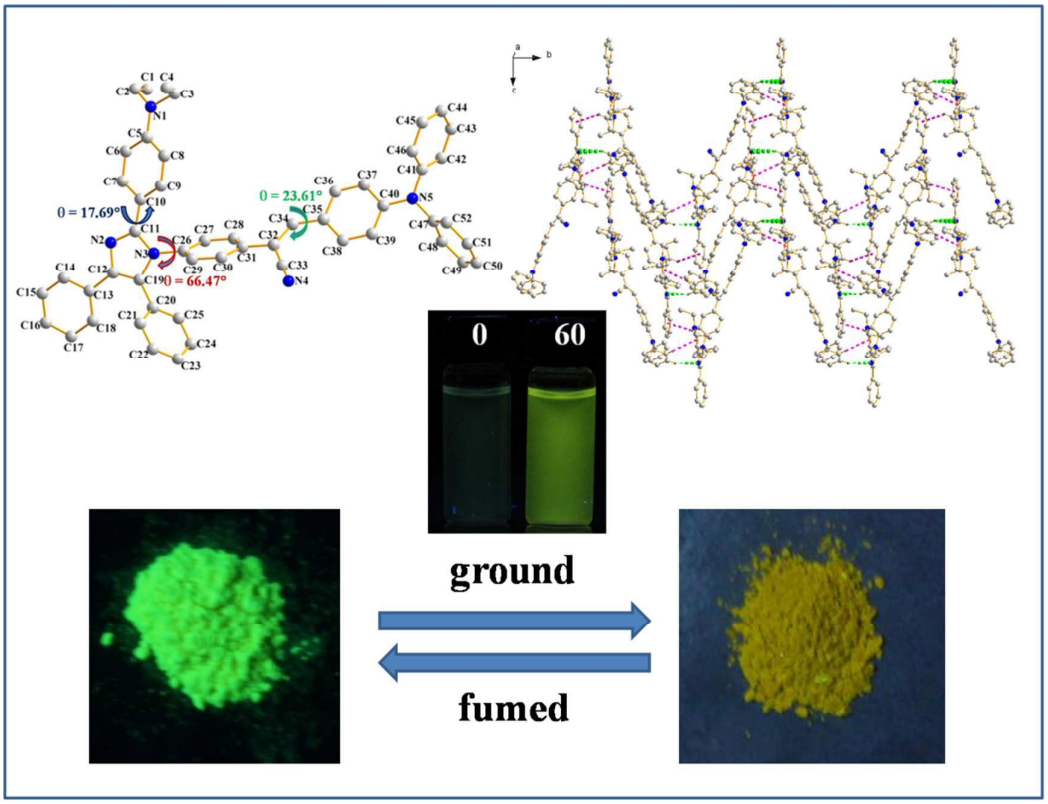

Twisted tetraphenyl imidazole derivatives functionalized by α-cyanostilbene possess aggregation-induced emission enhancement and mechanochromic luminescence properties.